

## **Distributed parameterization of a large scale water balance model for an Australian forested region**

**FRED G. R. WATSON**

*Department of Civil and Environmental Engineering, Cooperative Research Centre for Catchment Hydrology, University of Melbourne, Parkville, Victoria 3052, Australia*

**ROBERT A. VERTESSY**

*CSIRO Division of Water Resources, Cooperative Research Centre for Catchment Hydrology, GPO Box 1666, Canberra, Australian Capital Territory 2601, Australia*

**LAWRENCE E. BAND**

*Department of Geography, University of Toronto, Toronto, Ontario M5S 1A1, Canada*

**Abstract** The parameterization of a large-scale hydrological model (RHESSys) for a forested region is described. Using the GRASS GIS, a range of topographic, vegetative, climatic, and edaphic parameters were mapped over the region. A regional DEM was validated by ground-truthing and shown to give an excessively smooth representation of the terrain which influences moisture distribution predictions. LAI was mapped by regressing shade-corrected satellite imagery against ground-based measurements and applying the regression equations to the imagery. Precipitation was mapped using both elevation lapse rates and a more data-intensive 3D spline interpolation, the latter proving more appropriate. Areal estimates of soil properties were made through inverse determination from baseflow analysis but a regional distribution was not performed. These diverse improvements to previous parameterization techniques are discussed with respect to their likely effect on RHESSys operation.

### **INTRODUCTION**

A regional-scale, distributed-parameter, hydrological modelling study is under way in the forested central highlands of Victoria, Australia (Fig. 1). The study aims to model water yield from five, large, forested basins (total area 161 km<sup>2</sup>) and, in so doing, to explain the hydrological processes and external influences controlling water yield. A strong relationship is observed between water yield and forest age, which can be explained by high transpiration in regrowth forests. Evapotranspiration is controlled in part by soil moisture and leaf area so the heterogeneity of these variables is of key interest. Topography is also investigated as control of evapotranspiration (through radiation) as well as saturation excess surface runoff. Precipitation is the input to the water cycle so accurate mapping of its distribution is of paramount importance.

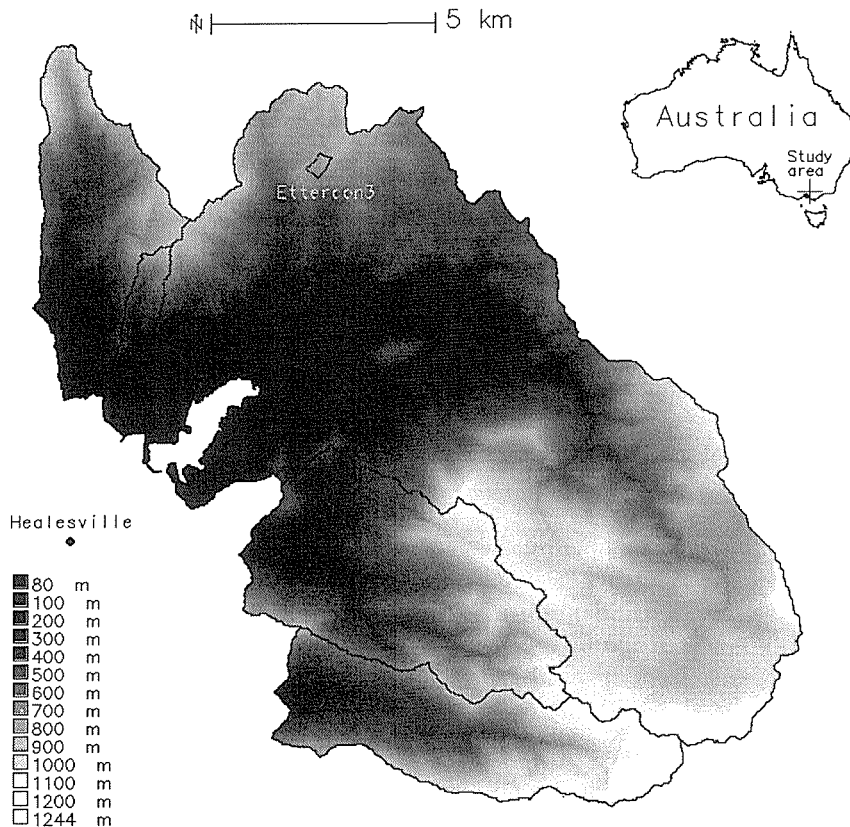


**Fig. 1** Location and elevation of the Maroondah region in southeastern Australia showing the five main water supply basins and one of the 17 experimental basins: Ettercon3.

## THE MODEL

The North American modelling system, RHESSys (Band *et al.*, 1993), is used to predict water yield and understand the processes by which it occurs. RHESSys operates in conjunction with the GRASS GIS (V. 4.1) and is a combination of previously developed models of hillslope hydrology, canopy hydrology and climate – TOPMODEL, FOREST-BGC, and MT-CLIM (Beven *et al.*, 1994; Running & Coughlan, 1988; Running *et al.*, 1987). RHESSys models hydrologically self-similar areas, defined according to a topography-soil index (*TSI*) as shown in equation (1):

$$TSI = \ln(aT_e / (T_i \tan \beta)) \quad (1)$$

where  $a$  is the up slope area per unit contour length (m),  $\beta$  is the slope gradient,  $T_i$  is the local soil transmissivity ( $\text{m}^2 \text{day}^{-1}$ ) and  $T_e$  is a measure of the mean value of  $T_i$ . If transmissivity is assumed to be homogeneous, we are left with an index of topography alone.

Lateral subsurface flow is modelled implicitly according to a distribution function based on the assumption that the saturated hydraulic conductivity of the soil declines exponentially with soil saturation deficit:

$$K = K_0 \exp(-S/m) \quad (2)$$

where  $K_0$  is the saturated hydraulic conductivity at the soil surface,  $S$  is the local saturation deficit and  $m$  is a shape parameter (note that  $T_i = K_0 m$ ). The distribution of hillslope saturated moisture can then be given as:

$$S = S' + m(\lambda - TSI) \quad (3)$$

where  $S'$  is the mean hillslope saturation deficit and  $\lambda$  is the mean value of the  $TSI$  assuming spatially constant transmissivity.

The required parameters for RHESys are leaf area index ( $LAI$ ), root zone water capacity,  $m$  from equations (2) and (3),  $K_0$  from equation (2), elevation, slope and aspect. The required climatic inputs are daily precipitation and temperature (max. and min.) at a base station.

## TOPOGRAPHIC INPUTS

Elevation, slope and aspect were estimated as a  $25 \times 25$  m gridded DEM (Fig. 1) fitted as a spline surface from 1:25 000 digital contour data. The contour data were constructed from air-photo interpretation (API).

The API DEM exhibited an excessively smooth representation of valley bottoms which was thought to significantly influence the prediction of wetted areas using equation (2). A ground-truthing exercise was undertaken to investigate the quality of the DEM and its effect on valley bottom smoothing. A detailed topographic survey of a small basin (Ettercon 3, 15 ha, Fig. 1) was made. Approximately 700 topographic points were surveyed and 25 m and 12.5 m DEMs were fitted to the data.

The extent of valley smoothing was assessed by taking sections across the basin from each DEM (Fig. 2). The two ground-surveyed DEMs present very similar cross-sections indicating that basins of this size are equally well represented by 25 and 12.5 m DEMs. The API DEM however, describes a significantly smoother cross-section. Representa-

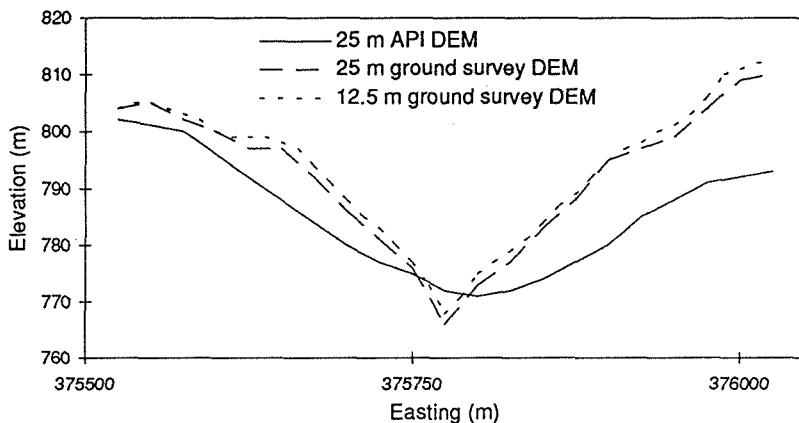


Fig. 2 Exaggerated cross-sections through three DEMs for the Ettercon3 experimental basin.

tion of forested basin topography at this scale using a DEM derived from air-photo interpretation is clearly not ideal.

The effect of valley smoothing on model behaviour was studied using a comparison between distributions of the  $\ln(a/\tan \beta)$  index as shown in Fig. 3(a). The distributions calculated using the ground surveyed DEMs are similar apart from a small shift towards higher values with increased grid size, a normal consequence of differing grid sizes (Quinn *et al.*, 1995). There is a much greater difference between the API DEM and the ground surveyed DEMs. Once again, this appears largely as a shift along the  $x$ -axis but a difference in shape is also apparent. The distributions calculated using the ground surveyed DEMs have longer, higher tails than the API DEM distribution. Beven & Wood (1983) state that such long, high tails imply a greater saturated area and hence a greater likelihood of saturation excess overland flow. However, the mean value of  $\ln(a/\tan \beta)$ ,  $\lambda$ , must also be taken into account.

A more thorough comparison of the effects of differing DEMs on model behaviour can be made by comparing distributions of  $S$  instead of  $\ln(a/\tan \beta)$ . Assuming homogeneous transmissivity, equation (3) shows that *net* shifts in  $\ln(a/\tan \beta)$  are cancelled by corresponding shifts in  $\lambda$ . Thus, in predicting soil moisture patterns, the *shape* of the

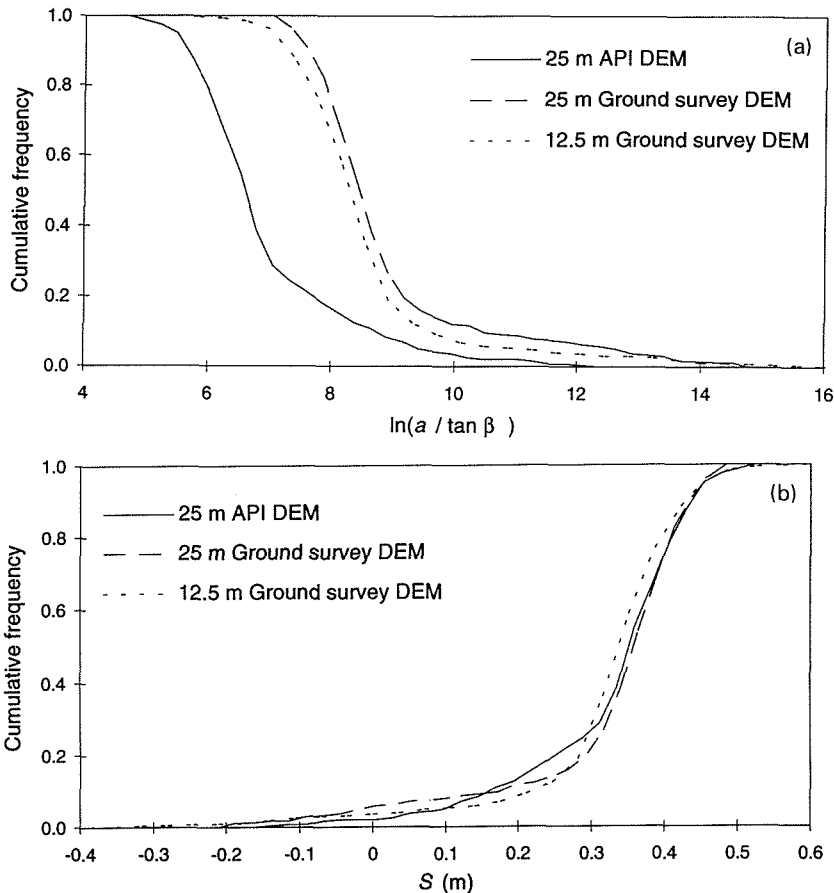


Fig. 3 Comparison of cumulative distributions of: (a) the  $\ln(a/\tan \beta)$  index and (b) predicted saturation deficit throughout the Ettercon3 basin.

$\ln(a/\tan \beta)$  is of greatest importance. Fig. 3(b) shows the  $S$  distribution predicted using each of the DEMs. For this exercise,  $m$  was taken as 0.09 and  $S'$  was calibrated such that the saturated proportion of the catchment predicted using the 12.5 m DEM was 3.6%, a typical value for the basin (Duncan & Langford, 1977). As expected, the three curves have been shifted such that they now overlap and a comparison of their relative shapes may be easily made. At  $S = 0$  m, the API DEM curve is lower than the curves derived from ground survey. Thus a greater saturated area would appear to be predicted using the ground surveyed DEMs, which is contrary to our initial expectations. It appears that whilst the API DEM represents a broader valley bottom and therefore greater opportunity for wetted area expansion, up slope areas are distributed more thinly over this broader area and saturation does not occur until further down the catchment. This explanation is confirmed in Fig. 3(b) by the prediction under the API DEM of a relatively high area of *near* saturation (at  $S = 0.25$  m).

## VEGETATION INPUTS

Leaf area index ( $LAI$ ) is a sensitive parameter strongly influencing precipitation interception, radiation interception and transpiration (Vertessy *et al.*, 1993).  $LAI$  is mapped for input to RHESSys by using ground-based measurements of  $LAI$  (Vertessy *et al.*, 1995) to calibrate multispectral satellite images of the region. Ratios between Thematic Mapper (TM) Bands 3, 4, and 5 have been used to estimate  $LAI$  (Nemani *et al.*, 1993). Here, an alternative approach is tested employing explicit shading correction as follows:

A vector forest type map developed using API and ground survey was co-registered to the  $25 \times 25$  m grid used in the study. The map delineated 8 forest types which form the spatial framework within which the  $LAI$ /sensing relationships are applied. A geocoded, 7-band TM image from February 1994 was obtained for the region. To correct a slight miss-registration against cartographic data, the image was re-registered by optimizing its correlation with a theoretical shading image derived from the DEM (see below) with respect to slight lateral coordinate shifts. The image was then corrected for topographic shading using the Minnaert method (Colby, 1991) which gave a correlation coefficient between modelled shading and the re-registered imagery (Band 4) of 0.71 ( $N = 260\ 531$ ). The shade-corrected imagery retained some unwanted cross-band features which were further corrected using band-ratioing applied to the *shade-corrected* imagery.

To generate the final  $LAI$  map, both uncorrected and shade-corrected Band 4/Band 3 maps were regressed against a total of 18  $LAI$  measurements from eight mountain ash (*Eucalyptus regnans*) sites made using a hand-held light meter. The regression on corrected data performed best with a correlation coefficient of  $R = 0.74$ . The regression equation was then applied to the imagery to generate an  $LAI$  map for areas forested with mountain ash. A roughly normal distribution of  $LAI$  values occurred with 5% and 95% bounds of around 1 and 6.  $LAI$  maps for the remaining seven forest types were computed by scaling the linear relationship determined for mountain ash according to estimated 5% and 95%  $LAI$  bounds for each forest type. Figure 4 shows the final  $LAI$  map — a composite of the maps for each forest type. Many aspects of Fig. 4 are intuitively correct, such as the lighter bands of riparian vegetation in the southeast, surrounded by a darker area representing a less verdant and more alpine forest species of the southeast

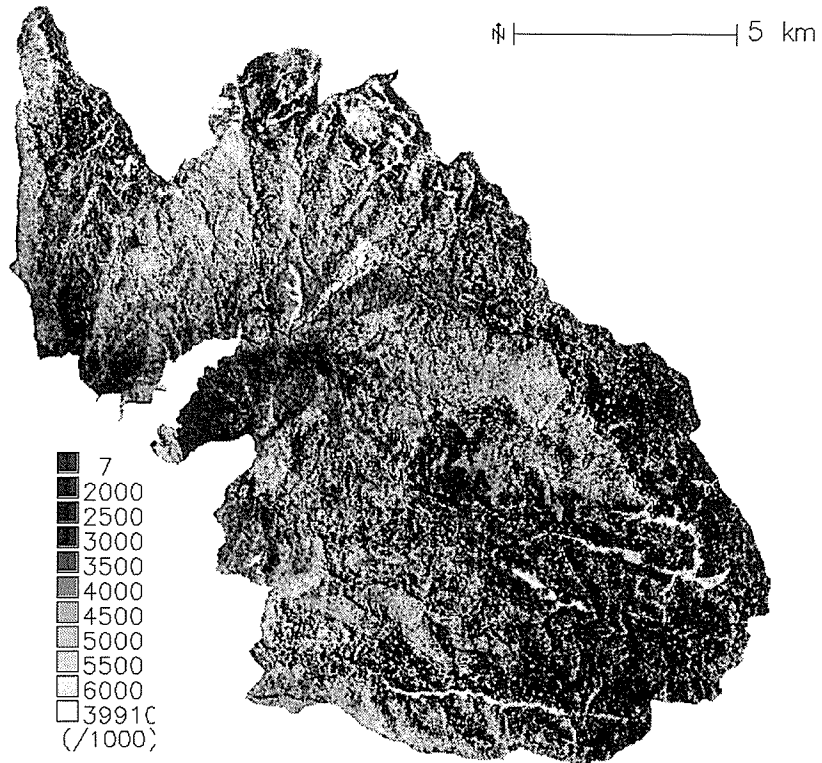


**Fig. 4** LAI map for the region calculated from regression of ground observations of LAI against remotely sensed TM satellite imagery.

plateau. Also, the dry, north-facing slopes to the south of Maroondah reservoir (in the mid-west of the region) are correctly mapped with low LAI.

## CLIMATIC INPUTS

Precipitation within RHESSys is estimated separately for each hillslope using the mean elevation of the hillslope to scale daily precipitation at some base station according to a supplied precipitation/elevation lapse rate. This method was tested against a more data intensive interpolation method which makes use of the 73 nearby precipitation gauging sites. For this exercise, 326 hillslopes with a mean area of 50 ha were defined for the region using the GRASS program *r.watershed*.

Precipitation records for the gauging sites are not all concurrent and often patchy. Comparisons between sites are thus influenced by inter-annual variability which was corrected by dividing all monthly totals by corresponding values from a central base station. The final precipitation data are expressed as mean monthly precipitation indices (MMPIs) relative to the mean base station precipitation. If we assume that the spatial pattern of mean monthly precipitation is constant throughout the year, only a single MMPI is required for each site.

A spline surface was fitted to the MMPI values with respect to their 3D location using the ANUSPLIN package. The three-dimensionality of this procedure enables not only the precipitation/elevation relationship to be modelled (as in RHESys) but also the variation in precipitation in the horizontal dimension – independent of elevation. The 3D spline surface and the corresponding surface calculated from a simple precipitation/elevation correlation were aggregated to give maps of MMPI at each hillslope (Fig. 5). A strong elevation influence is present in both part of the Figure but the differences show that horizontal influences are also strong in the region. The improved method (Fig. 5(a)) describes a pattern of very high precipitation over the southeastern plateau of the region whilst the northern ranges do not appear to receive precipitation in similar

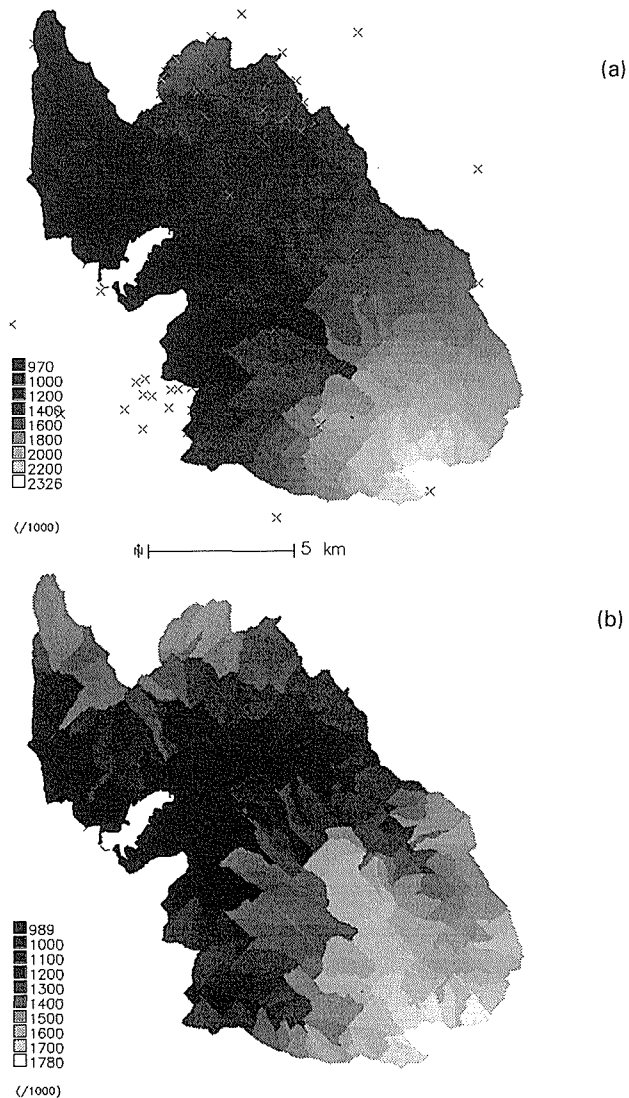


**Fig. 5** Hillslope-aggregated MMPI derived from: (a) a spline surface fitted to 73 sites; (b) linear regression of precipitation against elevation.

proportion to their high elevation. In Fig. 5(b), all areas of equal elevation are mapped with equal precipitation and the southeastern precipitation high is not represented.

## SOIL INPUTS

Problems are involved in scaling direct measurements of soil from the point scale to the grid cell scale and from the grid cell scale to entire regions. The latter requires a large number of measurements to enable an appropriate description of the relationship between soil properties and modelled environmental variables. An alternative method is inverse determination through baseflow analysis (Nathan & McMahon, 1990) which is described here for Ettercon3 (Fig. 1).

Beven *et al.* (1994) have shown that equation (2) leads to the following expression of hyperbolic baseflow recession over time:

$$\frac{1}{Q_b} = \frac{1}{Q_0} + \frac{t}{m} \quad (4)$$

where  $Q_b$  is the baseflow from the basin at time  $t$  since mean basin saturation and  $Q_0$  is the baseflow at mean basin saturation (treated as a calibration parameter here).

The key parameter in equation (4) is the shape parameter,  $m$ , which was determined by fitting equation (4) to observed baseflow recessions as follows. Lyne & Hollick's (1979) baseflow separation procedure was applied to 23 years of streamflow data for Ettercon3 and an individual recession segment was defined as a period of at least 21 days commencing at a peak in baseflow and continuing to the next rise. The 33 individual recessions so defined were assumed to follow a theoretical, master recession curve (MRC) of the form dictated by equation (4) which plots as a straight line on semi-inverse axes with slope  $m$ . The "best fit" MRC, and hence an estimate of  $m$ , is visually determined by automatically overlaying the individual recessions with MRCs of differing slopes until the best alignment between the two is found.

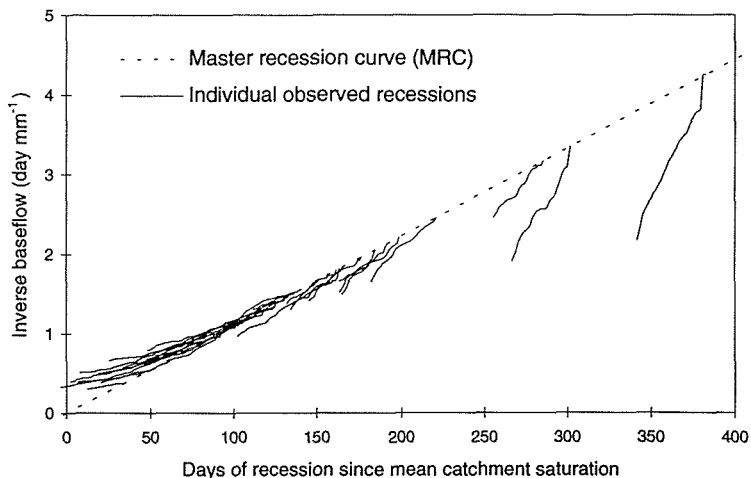


Fig. 6 Individual baseflow recessions from Ettercon3 aligned to a best fit MRC.

The best fit for Ettercon3 is shown in Fig. 6 ( $m = 0.09$ ). A poor fit is observed at high and low baseflow so boundary values were fitted ( $0.0075 < m < 0.17$ ). It was found that an exponential MRC fitted the data better than the hyperbolic MRC of equation (4). However, as the hyperbolic MRC is explicit in RHESys, it was retained pending the definition of a more appropriate model of basin response to subsurface flow. The regional heterogeneity of  $m$  will be addressed in future work using similar analyses for the other 16 small experimental basins in the region.

## DISCUSSION

GIS is a most valuable tool in helping to parameterize large scale, distributed hydrological models. The parameterization improvements presented here are highly inter-dependent, a feature made possible only through the use of a GIS. But with increased scale, complexity, and inter-dependence come pitfalls at every turn. Each of the techniques presented here has benefitted from a large fieldwork effort, and yet the primary avenue of further improvement for each would be to collect even more field data. For the hydrologist to acquire and develop more sophisticated GIS technology is a simple task compared to the data collection exercise which must be undertaken to satisfy the data needs of many new, large-scale, spatial modelling techniques. For the present study the next step is to conduct model sensitivity analyses which tell us *which data* to improve.

**Acknowledgement** This study was funded by the Cooperative Research Centre for Catchment Hydrology. We acknowledge the following: Sharon O'Sullivan (LAI data), Renuka Swaminathan (TM data), Keith Beven (TOPMODEL code), Tom McMahon, and all the survey staff holders.

## REFERENCES

- Band, L. E., Patterson, P., Nemani, R. & Running, S. (1993) Forest ecosystem processes at the watershed scale: incorporating hillslope hydrology. *Agric. For. Meteorol.* **63**, 93-126.
- Beven, K. J. & Wood, E. F. (1983) Catchment geomorphology and the dynamics of runoff contributing areas. *J. Hydrol.* **65**, 139-158.
- Beven, K. J., Lamb, R., Quinn, P., Romanowicz, R. & Freer, J. (1994) TOPMODEL. In: *Computer Models of Watershed Hydrology* (ed. by V. P. Singh). To be published by Water Resources Publ.
- Colby, J. D. (1991) Topographic normalization in rugged terrain. *Photogramm. Engng Rem. Sensing* **57**(5), 531-537.
- Duncan, H. P. & Langford, K. J. (1977) Streamflow characteristics. In: *First Progress Report – North Maroondah* (ed. by K. J. Langford & P. J. O'Shaughnessy), 215-229. MMBW Report no. MMBW-W-0005.
- Lyne, V. & Hollick, M. (1979) Stochastic time-variable rainfall-runoff modelling. In: *Hydrology and Water Resources Symp.* (Perth, September 1979), 89-92. Inst. Engrs Australia.
- Nathan, R. J. & McMahon, T. A. (1990) Evaluation of automated techniques for baseflow and recession analyses. *Wat. Resour. Res.* **26**, 1465-1473.
- Nemani, R., Pierce, L., Band, L. E. & Running, S. W. (1993) Forest ecosystem processes at the watershed scale: sensitivity to remotely sensed leaf area index observations. *Int. J. Rem. Sensing* **14**, 2519-2534.
- Quinn, P. F., Beven, K. J. & Lamb, R. (1995) The  $\ln(a/\tan\beta)$  index: how to calculate it and how to use it within the TOPMODEL framework. *Hydrol. Processes* **9**, 161-182.
- Quinn, P. F., Beven, K. J., Chevallier, P. & Planchon, O. (1991) The prediction of hillslope flow paths for distributed hydrologic modelling using digital terrain models. *Hydrol. Processes* **5**(1), 59-79.

- Running, S. W. & Coughlan, J. C. (1988) A general model of forest ecosystem processes for regional applications. I. Hydrologic balance, canopy gas exchange and primary production processes. *Ecol. Model.* **42**, 125-154.
- Running, S. W., Nemani, R. & Hungerford, R. D. (1987) Extrapolation of synoptic meteorological data in mountainous terrain and its use for simulating forest evapotranspiration and photosynthesis. *Can. J. For. Res.* **17**, 472-483.
- Vertessy, R. A., Benyon, R. G., O'Sullivan, S. K. & Gribben, P. R. (1995) Relationships between stem diameter, sapwood area, leaf area and transpiration in a young mountain ash forest. *Tree Physiol.* (in press).
- Vertessy, R. A., Hatton, T. J., O'Shaughnessy, P. J. & Jayasuriya, M. D. A. (1993) Predicting water yield from a mountain ash forest catchment using a terrain analysis based catchment model. *J. Hydrol.* **150**, 665-700.